11-2004

Signal-Strength Based Localization in Wireless Fading Channels

Aleksandar Dogandžić
Iowa State University, ald@iastate.edu

Prihamdhani P. Amran
Iowa State University

Signal-Strength Based Localization in Wireless Fading Channels

Abstract

We develop maximum likelihood (ML) methods for location estimation using spatio-temporal received-signal strength (RSS) measurements in wireless fading channels. Fading and composite fading-shadowing scenarios with completely unknown and partially known source signals are considered. We adopt gamma (Nakagami-m) and lognormal models to describe fading and shadowing effects, respectively. We also derive Cram´er-Rao bounds (CRBs) for the location parameters and discuss initialization of the proposed algorithms. Numerical simulations demonstrate the performance of our estimators.

Keywords

RSS, gamma, Nakagami-m, lognormal, Cramer-Rao bounds

Disciplines

Electrical and Computer Engineering | Signal Processing

Comments

This is a manuscript of a proceeding in *Conference Record of the Thirty-Eighth Asilomar Conference on Signals, Systems and Computers, 2004*: 2160. Posted with permission.

Signal-Strength Based Localization in Wireless Fading Channels

Aleksandar Dogandžić and Prihamdhani P. Amran
Department of Electrical and Computer Engineering
Iowa State University, 3119 Coover Hall, Ames, IA 50011
Email: ald@iastate.edu, prihamdhani@yahoo.com

***Abstract*— We develop maximum likelihood (ML) methods for location estimation using spatio-temporal received-signal-strength (RSS) measurements in wireless fading channels. Fading and composite fading-shadowing scenarios with completely unknown and partially known source signals are considered. We adopt gamma (Nakagami-m) and lognormal models to describe fading and shadowing effects, respectively. We also derive Cramér-Rao bounds (CRBs) for the location parameters and discuss initialization of the proposed algorithms. Numerical simulations demonstrate the performance of our estimators.**

I. Introduction

Location estimation is an important task in wireless cellular and sensor networks, see [1]–[8] and references therein. Most location technologies are based on time-of-arrival (TOA), time-difference-of-arrival (TDOA), angle-of-arrival (AOA), and received-signal-strength (RSS) measurements [1]–[4]. The RSS approach exploits signal attenuation with distance to determine the source location. This technique has been employed in both cellular and sensor networks (see [2] and [3]–[8], respectively) utilizing radio-frequency (RF) fading-channel [2]–[6] or acoustic measurements [3], [7], [8]. It is inexpensive compared with TOA/TDOA and AOA-based approaches,[1] and has been identified in [4] as the prime candidate for location estimation in wireless sensor networks.

Radio channels are affected by multipath fading and shadowing effects [3, ch. 4.4.1]. Most existing RSS localization methods for the RF scenario are based on spatial measurements and do not explicitly account for the fading effects, see [2] and [5]. A suboptimal averaging-window based method to mitigate the Rayleigh-fading effects is discussed in [6]. In this paper, we present maximum likelihood (ML) methods for RSS location estimation using *both* spatial and temporal RF measurements that follow

- a gamma (Nakagami-m) fading model[2] and
- a composite gamma-lognormal fading-shadowing model,

see [9, chs. 2.2.1.4 and 2.2.3]. The first (gamma) model can approximate well the acoustic-energy attenuation model in [7, Sect. 2.1] and is therefore applicable to the acoustic RSS scenario.

[1]Note that TOA/TDOA and AOA-based methods require accurate time-synchronization devices or costly antenna arrays (respectively) at each node in the network.

[2]The gamma model spans a wide range of fading conditions: it includes Rayleigh fading as a special case and can be used to closely approximate Ricean and Nakagami-q (Hoyt) fading scenarios, see [9, ch. 2.2.1.4].

In Sections II and III, we introduce the fading and composite fading-shadowing measurement models and propose ML estimation algorithms for these models (Sections II-A and III-A). Simulation results illustrating the performance of the proposed methods are presented in Section IV and concluding remarks are given in Section V.

II. Fading Measurement Model and Location Estimation

Assume that K nodes have been deployed in a wireless network at known locations $\boldsymbol{r}_k$, $k = 1, 2, \ldots, K$. At times $t = 1, 2, \ldots, N$, these nodes receive RSS measurements from a source having an unknown location $\boldsymbol{x}$. For simplicity, we focus on locating one source in a two-dimensional (2-D) network where $\boldsymbol{x}$ is described by two Cartesian coordinates; the proposed estimators can be easily extended to multiple source locations and a 3-D scenario. We assume that the source does not move significantly in the time frame $t \in \{1, 2, \ldots, N\}$ compared with the accuracy that we wish to achieve. The signal energies $y_k(t)$ received by the kth node at times $t = 1, 2, \ldots, N$ are modeled as independent gamma random variables with probability density functions (pdfs):

$$p_y(y_k(t)) = \frac{m_k^{m_k} y_k(t)^{m_k - 1}}{\big[a_k(\boldsymbol{x}) s(t)\big]^{m_k} \Gamma(m_k)} \exp\Big[-\frac{m_k y_k(t)}{a_k(\boldsymbol{x}) s(t)}\Big]$$

where

- m_k (known) Nakagami-m fading parameter corresponding to the channel between the source and the kth node;
- $s(t)$ *source-signal energy* at time t;
- $a_k(\boldsymbol{x})$ *signal-strength (path-loss) function* for the *k*th node.

Under the RF scenario, the above model accounts for the fading effects, where m_k describes the amount of fading between the source and the kth node. The non-line-of-sight fading condition at the kth node can be modeled using $m_k = 1$ (Rayleigh fading); a similar model was also discussed in [6]. The line-of-sight (Ricean) fading is accounted for by choosing $m_k > 1$, see [9, ch. 2.2.1.4]. Under the acoustic scenario, m_k quantifies the reliability of the received energy measurements at the kth node.

We adopt the following model for the signal-strength function (see [8]):

$$a_k(\boldsymbol{x}) = \frac{1}{1 + \beta \cdot [(\boldsymbol{r}_k - \boldsymbol{x})^T (\boldsymbol{r}_k - \boldsymbol{x})]^{\alpha}} \tag{1}$$

which is similar to the path-loss and acoustic-energy attenuation functions in [2], [3], [5], [6], and [7]. Here, "^{T}" denotes a transpose and α and β are *known* signal-strength function parameters.

The source-signal energies $s(t)$, $t = 1, 2, \ldots, N$ are modeled as deterministic constants that are

(i) **completely unknown** or

(ii) **partially known** (known up to a scaling factor s):

$$s(t) = s \cdot c(t),\ t = 1, 2, \ldots, N \tag{2}$$

where $c(t)$ is a known function[3].

The first model applies to both RF and acoustic measurement scenarios, whereas the second model is suited only to the RF scenario.

Our goal is to estimate the *unknown* 2-D source location vector $\boldsymbol{x}$ under the above measurement and source-signal models.

A. ML Location Estimation

We develop computationally efficient ML methods for estimating the unknown source location $\boldsymbol{x}$ under the above measurement and source-signal models. Define

$$\boldsymbol{d}_k(\boldsymbol{x}) = \frac{1}{a_k(\boldsymbol{x})} \cdot \frac{\partial a_k(\boldsymbol{x})}{\partial \boldsymbol{x}}. \tag{3}$$

1) Completely Unknown Source Signals: Consider first the scenario where the source-signal energies are *completely unknown.* We derive the following nested Fisher scoring (NFS) algorithm[4] for estimating $\boldsymbol{x}$:

$$\boldsymbol{x}^{(i+1)} = \boldsymbol{x}^{(i)} + \mathrm{CRB}_{\boldsymbol{x}}(\boldsymbol{x}^{(i)}) \cdot \frac{\partial L(\boldsymbol{x}^{(i)}, \widehat{\boldsymbol{s}}(\boldsymbol{x}^{(i)}))}{\partial \boldsymbol{x}} \tag{4}$$

where i is the iteration index and

$$\mathrm{CRB}_{\boldsymbol{x}}(\boldsymbol{x}) = \frac{1}{N}\Big\{\big[\sum_{k=1}^{K} m_k\, \boldsymbol{d}_k(\boldsymbol{x})\, \boldsymbol{d}_k(\boldsymbol{x})^T\big] - \big[\sum_{k=1}^{K} m_k \boldsymbol{d}_k(\boldsymbol{x})\big] \cdot \big[\sum_{k=1}^{K} m_k \boldsymbol{d}_k(\boldsymbol{x})^T\big] / \big(\sum_{k=1}^{K} m_k\big)\Big\}^{-1} \tag{5a}$$

$$\frac{\partial L(\boldsymbol{x}, \boldsymbol{s})}{\partial \boldsymbol{x}} = \sum_{k=1}^{K} m_k \left[\frac{\sum_{t=1}^{N}[y_k(t)/s(t)]}{a_k(\boldsymbol{x})} - N\right] \boldsymbol{d}_k(\boldsymbol{x}) \tag{5b}$$

are the CRB matrix and score vector for $\boldsymbol{x}$. Here,

$$\boldsymbol{s} = \big[s(1), s(2), \ldots, s(N)\big]^T \tag{6}$$

is the vector of unknown source-signal energies and

$$\widehat{\boldsymbol{s}}(\boldsymbol{x}) = \big[\widehat{s}(1, \boldsymbol{x}), \widehat{s}(2, \boldsymbol{x}), \ldots, \widehat{s}(N, \boldsymbol{x})\big]^T \tag{7a}$$

denotes the ML estimate of $\boldsymbol{s}$ for a fixed $\boldsymbol{x}$, where

$$\widehat{s}(t, \boldsymbol{x}) = \left(\sum_{k=1}^{K} \frac{m_k y_k(t)}{a_k(\boldsymbol{x})}\right) \Big/ \big(\sum_{k=1}^{K} m_k\big) \tag{7b}$$

for $s(t)$, $t = 1, 2, \ldots, N$. Note also that $\mathrm{CRB}_{\boldsymbol{x}}(\boldsymbol{x})$ does not depend on the source signals $\boldsymbol{s}$ and decreases proportionally with N as N grows.

[3]For example, we can select $c(t) = 1$ to describe a constant-modulus communication signal in a flat-fading scenario.

[4]Nested Newton-type algorithms are discussed in detail in [10, Sect. 2].

2) Partially Known Source Signals: We now focus on *partially known* source signals. First, define

$$z_k = \frac{1}{N} \sum_{t=1}^{N} \frac{y_k(t)}{c(t)}. \tag{8}$$

The NFS algorithm for this case is

$$\boldsymbol{x}^{(i+1)} = \boldsymbol{x}^{(i)} + \mathrm{CRB}_{\boldsymbol{x}}(\boldsymbol{x}^{(i)}) \cdot \frac{\partial L(\boldsymbol{x}^{(i)}, \widehat{s}(\boldsymbol{x}^{(i)}))}{\partial \boldsymbol{x}} \tag{9}$$

where

$$\frac{\partial L(\boldsymbol{x}, s)}{\partial \boldsymbol{x}} = N \sum_{k=1}^{K} m_k \left[\frac{z_k}{a_k(\boldsymbol{x}) s} - 1\right] \boldsymbol{d}_k(\boldsymbol{x}) \tag{10a}$$

$$\widehat{s}(\boldsymbol{x}) = \frac{\sum_{k=1}^{K} m_k\, z_k \,/ a_k(\boldsymbol{x})}{\sum_{k=1}^{K} m_k} \tag{10b}$$

are the score vector for $\boldsymbol{x}$ and ML estimate of the scaling factor s for a fixed $\boldsymbol{x}$, and $\mathrm{CRB}_{\boldsymbol{x}}(\boldsymbol{x})$ is given in (5a). Thus, the CRB matrix for $\boldsymbol{x}$ is the same for *both* completely unknown and partially known source-signal models.

Interestingly, if $m_1 = m_2 = \ldots = m_K = m$ (equal fading conditions), then m cancels out in (4) and (9), implying that we can find the ML estimates of $\boldsymbol{x}$ without knowing m.

III. Fading-Shadowing Measurement Model and Location Estimation

We introduce a measurement model that accounts for both fading and shadowing effects. Assume that the energy measurements $y_k(t)$ received by the kth node at times $t = 1, 2, \ldots, N$ are conditionally independent gamma random variables with the following pdfs:

$$p_{y|\gamma}(y_k(t) \,|\, \gamma_k) = \frac{m_k^{m_k} y_k(t)^{m_k - 1}}{[\exp(\gamma_k) s(t)]^{m_k}\, \Gamma(m_k)} \cdot \exp\left[-\frac{m_k y_k(t)}{\exp(\gamma_k) s(t)}\right] \tag{11}$$

where γ_k is proportional to the kth *shadow power* in decibels (corresponding to the channel between the source and the kth node) and $s(t)$ and m_k have been defined in Section II. We now model γ_k, $k = 1, 2, \ldots, K$ as independent, identically distributed (i.i.d.) Gaussian random variables with pdfs

$$p_\gamma(\gamma_k) = (2\pi\sigma_\gamma^2)^{-1/2} \cdot \exp\left\{-[\gamma_k - \ln a_k(\boldsymbol{x})]^2 / (2\sigma_\gamma^2)\right\} \tag{12}$$

where σ_γ is (unknown) *shadow standard deviation* and $a_k(\boldsymbol{x})$ are the signal-strength functions defined in (1).

Our goal is to estimate the source location $\boldsymbol{x}$ under the above measurement model and both completely unknown and partially known source-signal models.

A. ML Location Estimation

We first develop an expectation-maximization (EM) algorithm for computing the ML estimates of $\boldsymbol{x}$ under the completely unknown source-signal model (see Section III-A.1) and then show how it can be modified to account for partially known source signals (see Section III-A.2).

Define the vector of measurements collected by the kth sensor:

$$\boldsymbol{y}_k = [y_k(1), y_k(2), \ldots, y_k(N)]^T.$$

1) Completely Unknown Source Signals: In the case of completely unknown source signals, we define the vector of unknown parameters:

$$\boldsymbol{\theta} = [\boldsymbol{x}^T, \boldsymbol{s}^T, \sigma_\gamma^2]^T. \tag{13}$$

We treat the shadow powers γ_k, $k = 1, 2, \ldots, K$ as the *unobserved* (or missing) data and derive the following iteration between the expectation (E) and maximization (M) steps:

E Step: Compute

$$\begin{aligned} \gamma_k^{(i)} &= \mathrm{E}_{\gamma|y}\big[\gamma_k \,|\, \boldsymbol{y}_k;\, \boldsymbol{\theta}^{(i)}\big] && \text{(14a)} \\ [\exp(-\gamma_k)]^{(i)} &= \mathrm{E}_{\gamma|y}\big[\exp(-\gamma_k) \,|\, \boldsymbol{y}_k;\, \boldsymbol{\theta}^{(i)}\big] && \text{(14b)} \\ w_k(\boldsymbol{s}^{(i)}) &= \frac{1}{N}\sum_{t=1}^{N} \frac{y_k(t)}{s^{(i)}(t)} && \text{(14c)} \end{aligned}$$

for $k = 1, 2, \ldots, K$ and

$$(\overline{\gamma^2})^{(i)} = \frac{1}{K} \cdot \sum_{k=1}^{K} \mathrm{E}_{\gamma|y}\big[\gamma_k^2 \mid \boldsymbol{y}_k;\, \boldsymbol{\theta}^{(i)}\big] \tag{14d}$$

where $\boldsymbol{s}^{(i)} = [s^{(i)}(1), s^{(i)}(2), \ldots, s^{(i)}(N)]^T$ and

$$\boldsymbol{\theta}^{(i)} = [(\boldsymbol{x}^{(i)})^T, (\boldsymbol{s}^{(i)})^T, (\sigma_\gamma^2)^{(i)}]^T \tag{14e}$$

is the ith-iteration estimate of all the unknown parameters. Here, (14a), (14b), and (14d) are computed using (15), shown at the bottom of the page, with $f(\gamma_k) = \gamma_k, \exp(-\gamma_k)$, and γ_k^2, $k = 1, 2, \ldots, K$. The approximate expression in (15b) follows by applying Gauss-Hermite quadrature (GHQ) to numerically evaluate integrals in the numerator and denominator of (15a); here, L is the quadrature order and $q_l, h_l,\ l = 1, \ldots, L$ are the GHQ abscissas and weights, tabulated in e.g. [11].

M Step: Compute

$$s^{(i+1)}(t) = \frac{\sum_{k=1}^{K} m_k y_k(t)\,[\exp(-\gamma_k)]^{(i)}}{\sum_{k=1}^{K} m_k} \tag{16a}$$

for $t = 1, 2, \ldots, N$ and

$$\begin{aligned} (\sigma_\gamma^2)^{(i+1)} &= (\overline{\gamma^2})^{(i)} - \frac{2}{K}\sum_{k=1}^{K}[\gamma_k^{(i)} \ln a_k(\boldsymbol{x}^{(i)})] \\ &\quad + \frac{1}{K}\sum_{k=1}^{K}[\ln a_k(\boldsymbol{x}^{(i)})]^2 && \text{(16b)} \end{aligned}$$

and find $\boldsymbol{x}^{(i+1)}$ that maximizes

$$\begin{aligned} \boldsymbol{x}^{(i+1)} &= \arg\max_{\boldsymbol{x}} \Big\{ \sum_{k=1}^{K} [\gamma_k^{(i)}\ \ln a_k(\boldsymbol{x})] \\ &\quad -\frac{1}{2} \cdot \sum_{k=1}^{K} [\ln a_k(\boldsymbol{x})]^2 \Big\} && \text{(16c)} \end{aligned}$$

which can be efficiently performed using the Newton-Raphson iteration (see e.g. [12, ch. 9.5]).

2) Partially Known Source Signals: The above EM iteration can be easily modified to account for the partially known source-signal model: replace (14c) with [see also (8)]

$$w_k(s^{(i)}) = z_k / s^{(i)} \tag{14c'}$$

and (16a) with

$$s^{(i+1)} = \frac{\sum_{k=1}^{K} m_k\, z_k\, [\exp(-\gamma_k)]^{(i)}}{\sum_{k=1}^{K} m_k} \tag{16a'}$$

and keep the other steps in (14)–(16) intact. In this case, the vector of unknown parameters is

$$\boldsymbol{\theta} = [\boldsymbol{x}^T, s, \sigma_\gamma^2]^T. \tag{17}$$

3) Initialization: The above EM algorithms can be initialized by fitting a lognormal model to the time-averaged measurements

$$\overline{y}_k = \frac{1}{N}\sum_{t=1}^{N} y_k(t), \quad k = 1, 2, \ldots, K \tag{18}$$

which leads to

$$\begin{aligned} \boldsymbol{x}^{(0)} &= \arg\max_{\boldsymbol{x}} \Big\{ \Big[\sum_{k=1}^{K} (\ln \overline{y}_k - g) \cdot \ln a_k(\boldsymbol{x}) \Big] \\ &\quad -\frac{1}{2}\sum_{k=1}^{K}[\ln a_k(\boldsymbol{x})]^2 + \frac{1}{2K}\Big[\sum_{k=1}^{K} \ln a_k(\boldsymbol{x})\Big]^2 \Big\} && \text{(19)} \end{aligned}$$

where

$$g = \frac{1}{K}\sum_{k=1}^{K} \ln \overline{y}_k. \tag{20}$$

This estimator is outlined in [2, Sect. II] and a similar approach is discussed in [5]. We also propose the following initial estimate of σ_γ^2:

$$\begin{aligned} \widehat{\sigma}_\gamma^{(0)} &= \Big\{ \frac{1}{K}\sum_{k=1}^{K} [\ln \overline{y}_k - \ln a_k(\boldsymbol{x}^{(0)})]^2 \Big\} \\ &\quad - \Big[g - \frac{1}{K}\sum_{k=1}^{K} \ln a_k(\boldsymbol{x}^{(0)}) \Big]^2. && \text{(21)} \end{aligned}$$

$$\begin{aligned} \mathrm{E}_{\gamma|y}[f(\gamma_k) \,|\, \boldsymbol{y}_k; \boldsymbol{\theta}] &= \frac{\int_{-\infty}^{\infty} f(\gamma)\, \big[\prod_{t=1}^{N} p_{y|\gamma}(y_k(t) \,|\, \gamma)\big]\, p_\gamma(\gamma)\, d\gamma}{\int_{-\infty}^{\infty} \big[\prod_{t=1}^{N} p_{y|\gamma}(y_k(t) \,|\, \gamma)\big]\, p_\gamma(\gamma)\, d\gamma} && \text{(15a)} \\ &\approx \frac{\sum_{l=1}^{L} h_l\, f\big(\upsilon_l(\boldsymbol{x}, \sigma_\gamma^2, k)\big)\, \exp\Big(- m_k N \cdot \{\upsilon_l(\boldsymbol{x}, \sigma_\gamma^2, k) + \exp[-\upsilon_l(\boldsymbol{x}, \sigma_\gamma^2, k)]\, w_k(\boldsymbol{s})\}\Big)}{\sum_{l=1}^{L} h_l\, \exp\Big(- m_k N \cdot \{\upsilon_l(\boldsymbol{x}, \sigma_\gamma^2, k) + \exp[-\upsilon_l(\boldsymbol{x}, \sigma_\gamma^2, k)]\, w_k(\boldsymbol{s})\}\Big)} && \text{(15b)} \end{aligned}$$

where

$$\upsilon_l(\boldsymbol{x}, \sigma_\gamma^2, k) = (2\sigma_\gamma^2)^{1/2} \cdot q_l + \ln \boldsymbol{a}_k(\boldsymbol{x}), \quad l = 1, 2, \ldots, L. \tag{15c}$$

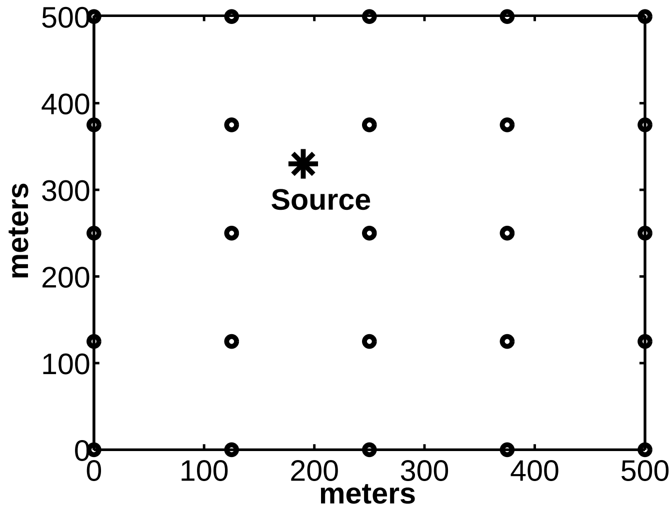

Fig. 1. A sensor network with $K = 25$ nodes.

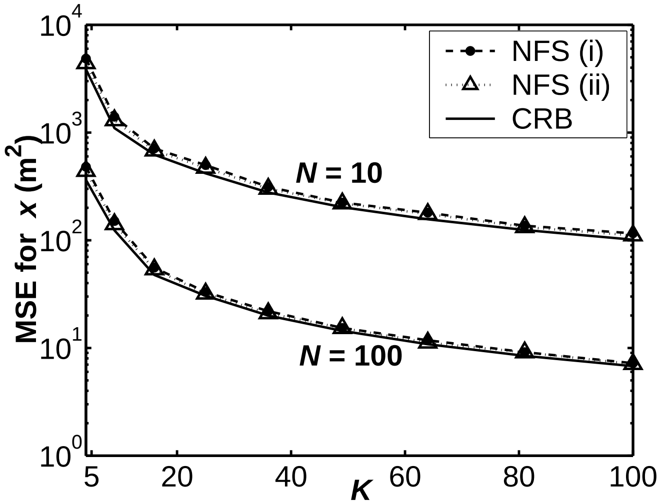

Fig. 2. MSEs for the NFS estimates of $\boldsymbol{x}$ as functions of the number of nodes K under the fading measurement scenario with $N \in \{10, 100\}$.

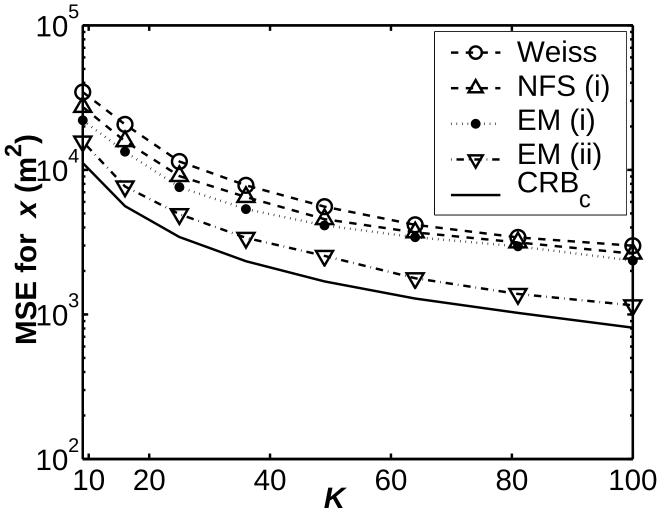

Fig. 3. MSEs for the EM and NFS estimates of $\boldsymbol{x}$ as functions of K under the fading-shadowing scenario with $N = 5$.

4) Cramér-Rao Bounds: Closed-form CRB expressions for the unknown parameters cannot be found for the composite fading-shadowing scenario. However, closed-form CRB for $\boldsymbol{x}$ exists under the *complete-data model* (assuming *known* shadow powers):

$$\mathrm{CRB}_{\mathrm{c},\boldsymbol{x}} = \sigma_\gamma^2 \cdot \big[\sum_{k=1}^{K} \boldsymbol{d}_k(\boldsymbol{x})\boldsymbol{d}_k(\boldsymbol{x})^T\big]^{-1}. \tag{22}$$

Clearly, the above complete-data CRB is a lower bound on the exact $\mathrm{CRB}_{\boldsymbol{x}}$, i.e. $\mathrm{CRB}_{\boldsymbol{x}} - \mathrm{CRB}_{\mathrm{c},\boldsymbol{x}}$ is a positive semidefinite matrix. Note that $\mathrm{CRB}_{\mathrm{c},\boldsymbol{x}}$ is proportional to the shadow variance σ_γ^2 and does not depend on N.

IV. Numerical Examples

We evaluate the estimation accuracy of the proposed methods. Consider a sensor-network scenario with nodes uniformly distributed in a square region measuring 500×500 m^2, as depicted in Fig. 1. Our performance metric is the mean-square error (MSE) of an estimator, calculated using 2000 independent trials. Here, we present *total MSEs* for the location estimates:

$$\mathrm{MSE}_x = \mathrm{MSE}_{x_1} + \mathrm{MSE}_{x_2}, \quad \boldsymbol{x} = [x_1, x_2]^T$$

averaged over random source locations $\boldsymbol{x}$ uniformly distributed within the network area. In all examples, we have chosen the Rayleigh-fading scenario, i.e.

$$m_1 = m_2 = \ldots = m_K = 1$$

and the following signal-strength function parameters: $\alpha = 1$ and $\beta = 0.0001$. The source-signal energies were generated using i.i.d. samples corresponding to the 16 quadrature amplitude modulation (QAM) modulation scheme with equiprobable symbols.

The first set of simulation results is presented in Fig. 2. We focus on the fading scenario described in Section II and apply the NFS algorithms for completely unknown and partially known source-signal models in (4) and (9), denoted by NFS (i) and NFS (ii), respectively. Fig. 2 shows the MSEs (and corresponding CRBs) for the obtained estimates of the source locations as functions of the number of nodes K, where $N \in \{10, 100\}$. Note that the CRBs for $\boldsymbol{x}$ are the same under both source-signal models (see Section II-A) and the corresponding MSEs are also approximately equal.

We now consider the fading-shadowing scenario with $\sigma_\gamma = 1$ (corresponding to the shadow standard deviation of 4.3 dB, which is typical in radio channels [13, ch. 2.4]) and apply the EM algorithms for completely unknown and partially known source-signal models, denoted by EM (i) and EM (ii) (respectively). The EM algorithms were initialized using the Weiss's estimator in (19). In Figs. 3, 4, and 5, we present the MSEs (and corresponding CRBs) for the EM (i), EM (ii), Weiss's, and NFS (i) estimates of $\boldsymbol{x}$ as functions of K,

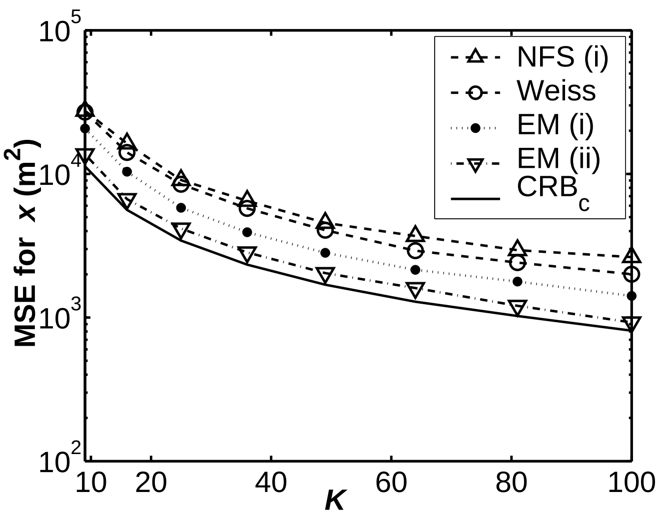

Fig. 4. MSEs for the EM and NFS estimates of $\boldsymbol{x}$ as functions of K under the fading-shadowing scenario with $N = 10$.

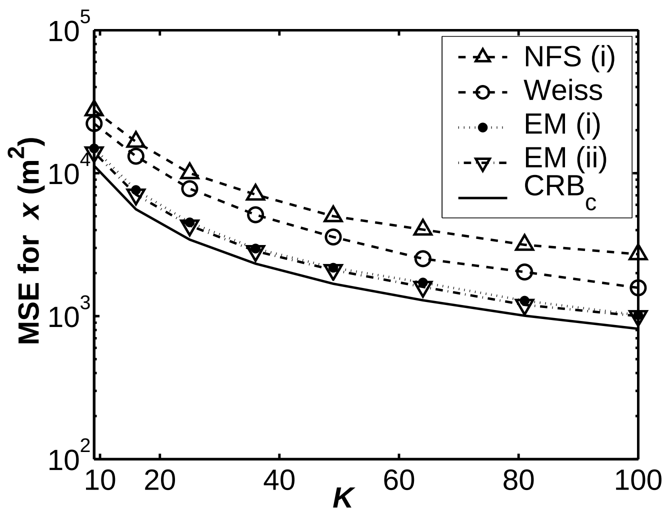

Fig. 5. MSEs for the EM and NFS estimates of $\boldsymbol{x}$ as functions of K under the fading-shadowing scenario with $N = 100$.

where $N = 5, 10$, and 100, respectively. The maximization in (16c) was performed using the Newton-Raphson algorithm. The EM algorithm for partially known source signals [EM (ii)] outperforms other methods and achieves MSEs close to the corresponding complete-data CRBs. As expected, the EM algorithm for completely unknown source signals [EM (i)] approaches the performance of the EM (ii) algorithm as the number of time samples N grows.

Under the above fading-shadowing scenario, the NFS method outperforms the Weiss's estimator when N is small (see Fig. 3); however, the Weiss's estimator is better for larger values of N (see Figs. 4. and 5). Furthermore, the results in Figs. 3–5 imply that the NFS method does not improve as N increases.

V. Concluding Remarks

We derived maximum likelihood methods for location estimation in fading and fading-shadowing wireless channels. Further research will include developing distributed localization algorithms for sensor-network applications.

References

[1] A.H. Sayed and N. Yousef, "Wireless location," in *Wiley Encyclopedia of Telecommunications*, J.G. Proakis (Ed.), New York: Wiley, 2003.

[2] A.J. Weiss, "On the accuracy of a cellular location system based on RSS measurements," *IEEE Trans. Veh. Technol.*, vol. 52, pp. 1508–1518, Nov. 2003.

[3] F. Zhao and L.J. Guibas, *Wireless Sensor Networks: An Information Processing Approach*, San Francisco, CA: Morgan Kaufmann, 2004.

[4] C. Savarese, J.M. Rabaey, and J. Beutel, "Locationing in distributed ad-hoc wireless sensor networks," in *Proc. Int. Conf. Acoust., Speech, Signal Processing*, Salt Lake City, UT, May 2001, pp. 2037–2040.

[5] N. Patwari, A.O. Hero, and M. Perkins, "Relative location estimation in wireless sensor networks," *IEEE Trans. Signal Processing*, vol. 51, pp. 2137–2148, Aug. 2003.

[6] P. Bergamo and G. Mazzini, "Localization in sensor network with fading and mobility," in *Proc. 13th IEEE Int. Symp. PIMRC*, Lisbon, Portugal, Sept. 2002, pp. 750–754.

[7] X. Sheng and Y.-H. Hu, "Energy based acoustic source localization," in *Proc. 2nd Int. Workshop Information Processing Sensor Networks*, Palo Alto, CA, Apr. 2003, pp. 285–300.

[8] R. Niu and P.K. Varshney, "Target location estimation in wireless sensor networks using binary data," in *Proc. Int. Conf. Acoust., Speech, Signal Processing*, Montreal, Que., Canada, May 2004, pp. 1026–1031.

[9] M.K. Simon and M.-S. Alouini, *Digital Communication Over Fading Channels*, New York: Wiley, 2000.

[10] G.K. Smyth, "Partitioned algorithms for maximum likelihood and other non-linear estimation," *Stat. Comput.*, vol. 6, pp. 201–216, Sept. 1998.

[11] *Handbook of Mathematical Functions with Formulas, Graphs, and Mathematical Tables*, New York: Dover, 1972, M. Abramowitz and I.A. Stegun (Eds.).

[12] S. Boyd and L. Vandenberghe, *Convex Optimization*, New York: Cambirdge Univ. Press, 2004.

[13] G. Stüber, *Principles of Mobile Communication*, 2nd. ed., Norwell, MA: Kluwer, 2001.